Application of Quantitative Structure−Activity Relationships to the Modeling of Antitubercular Compounds. 1. The Hydrazide Family

Cristina Ventura[†,‡] and Filomena Martins*[,†]

Departamento de Química e Bioquímica, Faculdade de Ciências, Universidade de Lisboa and Centro de Química e Bioquímica (CQB), Ed. C8, Campo Grande, 1749-016 Lisboa, Portugal, and Instituto Superior de Educação e Ciências, Alameda das Linhas de Torres, 179, 1750 Lisboa, Portugal

Received August 23, 2007

A QSAR/QSPR methodology was used to analyze a set of 173 hydrazides, a great part of which are isoniazid (INH) derivatives. Nineteen molecular descriptors of various types (physicochemical, steric, geometrical, and electronic) have been systematically tested through a careful application of MLR. The analysis revealed that the biological activity of these compounds against *M. tuberculosis* does not depend on lipophilicity, as measured by log *P*. Properties that account for the biological response of isoniazid and related compounds, consistent with a mechanism involving the formation of radical species, were identified. The role of substituents in the stabilization of the intermediate species that gives rise to the active agent, the acyl radical, is discussed. It is postulated that the activation of INH derivatives' prodrugs (hydrazines and hydrazones) occurs near the surface of *M. tuberculosis*.

Introduction

Tuberculosis (TB[a]) has become a harsh worldwide problem: about 2 million people die each year, particularly in developing countries; it is estimated that about one-third of the world population is currently infected with the bacillus in its latent form and that nearly 9 million new cases develop each year.[1,2] According to WHO, multiresistant tuberculosis is responsible for approximately 460 thousand new cases per year and for about 740 thousand new patients infected by both *M. tuberculosis* and HIV/AIDS.[3] Recent estimates show that 10% of all new TB infections are resistant to at least one anti-TB drug. Latest reports on multidrug resistant (MDR) and extensively drug-resistant tuberculosis (XDR-TB) indicate that rates of drug resistance may be much higher than previously described.[4]

The Stop Tuberculosis Partnership, a wide network of organizations, donors, and countries, has recently launched the Global Plan TO STOP TB 2006–2015,[3,4] an ambitious strategy that foresees a fall in the incident rates of all forms of TB by 2015, as a way to attain the Partnership's long-term target of eliminating tuberculosis as a public health problem by 2050. To achieve these goals, it is crucial, among other aspects, to invest in new tools, i.e., to develop (and adopt) new diagnostic tests, new drugs, and new vaccines.

To accomplish these objectives, basic research in molecular biology and microbiology directed toward the identification and validation of new targets for drugs and new candidate compounds, the development of new drugs and of more effective clinical trials, and a further (and deeper) knowledge of the mechanisms of action of existing (and future) active compounds are urgently sought and are therefore areas of strategic importance.

In the past 30 years, several proposals intended at understanding the mechanism of action of various drugs, in particular of compounds with the hydrazide functionality (R_1R_2-N-N-R_3R_4), against *M. tuberculosis*, have been presented in the literature.[5–19] However, the knowledge of these mechanisms of action is still rather limited.

It is generally accepted that any pharmacological process occurs in three conceptual steps: penetration, binding, and activation.[20] That being so, for an ideal drug to be efficient, it is crucial that it possesses adequate hydrophilic/hydrophobic properties to penetrate the biological system (be it a membrane, an organelle, a cell, an organ, or an organism), that it holds certain structural, geometrical, and/or physicochemical characteristics that allow it to bind to the biological target (enzyme, receptor, transporter, etc), and finally that the adduct formed produces a biological response that will generate an observable effect. Such a challenge, ubiquitous in the design of any new drug, implies some knowledge of structure–activity and, in general, of property−activity relationships.

Within our research group, a database has been assembled with more than 1700 potentially active compounds against *M. tuberculosis*, their respective biological activity expressed in terms of minimum inhibitory concentrations, MICs, as well as a large set of molecular descriptors and properties (Abraham's and Verloop's parameters, partition coefficients, geometrical and electronic parameters, etc.).

The purpose of the present paper is to initiate a systematic analysis of the main factors influencing the activity of each family of potential antitubercular compounds included in the referred database. Our first target compounds are those possessing a hydrazide functionality.

Materials and Methods

In this paper, we have analyzed 173 hydrazides whose structures are given in Table S1 in Supporting Information.

Abraham's descriptors[21] were calculated using the Absolv program. Partition coefficients were collected from Leo and Hansch's database as clogP [22] and MIC values from ref 11 (in a

* To whom correspondence should be addressed. Phone: (351) 217500870. Fax: (351) 217500088. E-mail: filomena.martins@fc.ul.pt.

[†] Faculdade de Ciências, Universidade de Lisboa and Centro de Química e Bioquímica (CQB).

[‡] Instituto Superior de Educação e Ciências.

[a]Abbreviations: TB, tuberculosis; *M. tuberculosis*, *Mycobacterium tuberculosis*; MDR, multidrug-resistant; XDR-TB, extensively drug-resistant tuberculosis; MIC, minimum inhibitory concentration; MLR, multiple linerar regression; LOO, leave-one-out; LMO, leave-many-out; INH, isoniazid; CP-KatG, catalase peroxidase of *M. tuberculosis*; NAD^+, nicotinamide adenine dinucleotide; NADH, reduced form of NAD^+; *mt*CP, *M. tuberculosis* catalase peroxidase.

10.1021/jm701048s CCC: $40.75
Published on Web 01/05/2008

total of 136 compounds tested against the BCG strain of *M. tuberculosis*) and from refs 12 and 23−25 (the remaining 37 compounds, tested against the $H_{37}R_v$ strain of the bacillus). Geometrical, structural, and electronic parameters were calculated using Molecular Modeling Pro Plus software,[26] after molecular structure optimization for each compound achieved by MM2, a molecular mechanics method incorporated in the software. Partial charges were calculated using the Del Re method and the MOPAC and CNDO programs and dipole moments either by PEOE and Huckel/4 methods or by a modified Del Re method, all included in the referenced software.

To establish a relationship between a property of the system and the molecular characteristics of the selected compounds, we performed standard multiple linear regressions (MLR) of the type

$$\mathbf{Y} = \mathbf{A}\mathbf{X} + \zeta \qquad (1)$$

where ζ is an $n \times 1$ residuals vector whose elements are assumed to be independent normal random variables with mean zero and known variance σ^2, $\mathbf{X}$ is a known $n \times k$ matrix of molecular descriptors, $\mathbf{A}$ is a $k \times 1$ vector of adjusted parameters, and $\mathbf{Y}$ is an $n \times 1$ vector of the response variable related to either the activity or other system property. For this purpose, we used the Data Analysis add-in, available in Microsoft Excel, and several statistical validation tests to ensure the reliability of the analyses.

The success of this type of methodology depends, however, on the fulfillment of essential prerequisites to guarantee the robustness and the interpretative and predictive abilities of the developed models. Homogeneity and representative character of the data set, redundancy of explanatory variables, and validation processes of the regression equations are issues that necessarily have to be addressed to ensure the reliability of the resulting information and/or the prediction capability of the model.

Searching for Outliers. Suspicious points were initially spotted by inspection of a plot of Y_{exp} vs Y_{calc}. The decision to consider any given point as an outlier was made according to two criteria: Cook's distance and the more conventional measure $|Y_{calc} - Y_{exp}| > 2$ SD, where SD stands for standard deviation of the fit.

Cook's distance,[27,28] D_i, is a measure of the influence of a suspicious point (outlier) in the results of a certain regression and is given by the following expression:

$$D_i = \frac{\sum_i (\hat{\Upsilon} - \hat{\Upsilon}_i)^2}{k\sigma^2} \qquad (2)$$

where $\hat{\Upsilon}$ and $\hat{\Upsilon}_i$ are the $n \times 1$ vectors of the predicted observations for the full data set and for the data set without the *i*th observation, respectively, and k is the number of parameters adjusted by the linear model with a variance σ^2. The specific criterion used to exclude an alleged outlier was $D_i > 4/(n - k - 1)$, where n is the number of observations.

The selected data set (i.e., without the outliers identified in the previous step) was then further tested using normal probability residual distribution plots, and the model was subsequently refitted.[29]

Internal Validation. When the outliers were excluded, the observations were divided into training and test sets with similar degrees of variability. In order to make an internal validation of the data, we applied the leave-one-out (LOO) approach to the training set:[30,31]

$$Q^2 = 1 - \frac{\sum_{i=1}^{\text{training}} (y_i - \hat{y}_i)^2}{\sum_{i=1}^{\text{training}} (y_i - \bar{y}_i)^2} \qquad (3)$$

where y_i, $\hat{y}_i$ and $\bar{y}_i$ are the measured, predicted, and averaged (over the whole data set) values of the dependent variable, respectively, and Q^2 is a cross-validated correlation coefficient.

The training set was also validated by the leave-many-out (LMO) approach. In this case, the training set was divided into n subsets T_i, being each $(n - 1)T_i$ subset taken as a training set and the whole remaining set as the test set. An average value of Q^2 (eq 3) for all the n trials was then determined. A high average value for Q^2 for the LMO validation gives an indication of the robustness of the model.

We have also considered traditional statistical criteria such as the determination coefficient, R^2, the standard deviation SD, the F statistic, and the significance level (SL) of each adjusted parameter (parameters were kept if SL > 98%) and have tested the intercorrelations among all descriptors included in each regression.

External Validation. The most serious way to assess a model's true predictive power is by using external validation, i.e., by making predictions for an independent data set not used to establish the model.

In our case, the test set used for external validation was chosen so that it fulfilled the same variability requisites as the training set, both in the independent and in the dependent variables.

The predictive ability of the model was assessed by an external Q^2_{ext} parameter defined as

$$Q^2_{ext} = 1 - \frac{\sum_{i=1}^{\text{test}} (y_i - \hat{y}_i)^2}{\sum_{i=1}^{\text{test}} (y_i - \bar{y}_{\text{training}})^2} \qquad (4)$$

where y_i and $\hat{y}_i$ are the measured and predicted (over the test set) values, respectively, and $\bar{y}_{\text{training}}$ is the averaged value of the dependent variable for the training set.

The following statistical criteria were also taken into consideration:[30,31]

$$Q^2_{ext} > 0.5; \quad R^2 > 0.6; \quad \frac{R^2 - R_0^{\,2}}{R^2} < 0.1; \quad 0.85 < m < 1.15$$

where R^2 is the test set's regression determination coefficient, $R_0^{\,2}$ is the same quantity for the regression that goes through the origin, and m is the slope of the regression between the estimated and the observed values. To further assess the predictive capability of the established QSAR and QSPR model equations, we have also computed three measures of fit: the average error (AE), the absolute average error (AAE), and the standard deviation (or rmse) of the predictions.

Results and Discussion

Hydrophobic/Hydrophilic Properties. As stated before, it is very important to be able to assess a compound's hydrophilic/hydrophobic character to anticipate its potential ability to penetrate a biological membrane. We have thus investigated the relationship between the lipophilicity of these compounds, as measured by their *n*-octanol/water partition coefficient, log *P*, in fact Leo and Hansch's clogP, and 19 molecular descriptors, X_i, of physicochemical, steric, geometrical, and electronic nature. With this purpose, we analyzed, for the 82 isoniazid derivatives, all multiple linear regressions of log *P* vs X_i which resulted from all possible combinations of the available descriptors for these compounds. We used the same methodology to relate log *P* with the 9 descriptors available for the 149 hydrazides for which we possess Abraham's parameters. Finally, we tested log *P* for the total set in terms of the 4 descriptors available for all 173 compounds.

A first analysis of the results, based on basic statistical criteria, showed that only the following types of relations were meaningful:

$$\log P = f(A,B,V,S,E) \qquad (5)$$

$$\log P = g(L,B_1,B_5,d_K) \qquad (6)$$

$$\log P = h(d_1,d_2,d_3,d_4,a_1,a_2,a_3,a_4,c,\mu) \qquad (7)$$

Equation 5 involves Abraham's physicochemical descriptors;[32] namely, A is the solute H-bond acidity, B is the solute H-bond basicity; V is the McGowan characteristic molar volume, S is the solute dipolarity/polarizability, and E is the excess molar refraction. These parameters were calculated by the Absolv program and are listed in Table 1.

Equation 6 entails the steric Verloop's parameters[33,34] L, B_1, and B_5 and a geometrical parameter d_K. B_1 is essentially a measure of the size (largely a steric effect) of the first atom in the substituent. B_5 is an attempt to define the effective volume of the whole substituent, and L is a measure of the substituent's length. d_k is the 2D distance between the pyridinic nitrogen and the terminal nitrogen of the hydrazide functionality[11] (see Figure 1).

These parameters were calculated using the Molecular Modeling Pro Plus software,[26] which optimizes a compound's molecular structure by MM2, a molecular mechanics method, and are shown together with the molecules' dipole moment, μ, in Table 2.

Equation 7 involves geometrical and electronic descriptors for the isoniazid derivatives, also calculated by Molecular Modeling Pro Plus. The a_4 parameter is the dihedral angle RNN(CO). c is the Mulliken charge on the external hydrazide N atom, and μ is, as stated above, the molecule's dipole moment. The remaining parameters are identified in Figure 1. All these descriptors, except for μ, are presented in Table 3.

For each multiple linear regression of eqs 5− 7, we tested every $C^m{}_p$ combination, where m is the number of descriptors in each equation and p varies from 1 to m. The best found MLR of eqs 6 and 7 shows rather low determination coefficients: $R^2 = 0.282$ (for $n = 105$) and $R^2 = 0.292$ (for $n = 78$), respectively.

No other multiparametric regression involving these descriptors and tested for any subset of compounds or for sets of compounds chemically related led to any statistically significant correlation. It seems therefore clear that the selected steric, geometrical, and electronic parameters do not seem to be capable of modeling the partition coefficient of these compounds in the n-octanol/water system. On the contrary, the best found MLR of eq 5 shows a much higher statistical significance:

$$\log P = (-2.012 \pm 0.161)B + (-0.553 \pm 0.126)S + (2.736 \pm 0.164)V \quad (8)$$

$$n = 149; \quad R^2 = 0.680; \quad SD = 0.994; \quad F = 104$$

It is interesting to observe that the coefficients of this equation have the same sign but are slightly different in magnitude from those previously reported by Abraham et al.[32b] in a correlation equation involving 493 compounds related to our set. This difference in magnitude might simply be due to the fact that our set of hydrazides occupies a different chemical space.

Since this equation seems to fairly explain the system's response in terms of log P, we attempted to validate the model both internally and externally in order to ensure its robustness and evaluate its predictive ability.[29–31] The results are shown in Table 4 and Figure 2. The predictions for the test set are expressed as standard deviation (SD), average error (AE), and average absolute error (AAE). The figures of merit fulfill the statistical criteria set above for both internal and external validation. We can therefore say that our model equation is capable of predicting log P for this class of compounds with an SD of 0.67 log units.

These results reveal that increasing the molar volume of the hydrazides favors the partition toward the organic component of the two-phase system while an increase in the solute's basicity and dipolarity/polarizability diminishes its presence in octanol.

It is interesting to note that, while these descriptors, in particular B and V, do explain a significant amount of the log P variability, whether we analyze the total set of compounds (eq 8) or different families separately, for the same sets there is again no significant correlation between either log P and the Verloop descriptors or between log P and any other group of geometrical or electronic descriptors. This seems to indicate that going from the aqueous to the organic phase depends more on the eventual ability of n-octanol to accommodate the solute through physicochemical interactions than on steric constraint or other geometrical characteristics of the solute.

On the other hand, it should also be noted that the inclusion of a third descriptor S, statistically significant for a 95% confidence level according to an F test of variances for the additional term, does not increase appreciably the quality of the regressions. This fact suggests that the dipolarity/polarizability characteristics of the solutes are not relevant for the partition process, although the relative importance of this parameter is higher when one considers the isoniazid derivatives separately (see Table 4).

The criterion used for the detection of outliers has excluded from the initial set ($n = 149$), a subset of 12 compounds located in the extremes of the dependent variable's domain, i.e., a subset of highly lipophilic and highly hydrophilic compounds (log $P_{\text{aver}} = -2.88$ for 11 out of the 12 outliers and log $P = 5.24$ for the remaining compound). (We considered outliers compounds **26**, **33**, **35**, **60**, **87**, **88**, **89**, **98**, **127**, **146**, **149**, and **173** in Table S1 in Supporting Information.) If we look at their molecular structures, we see that they correspond to compounds with high dipole moments and large dipolarity/polarizability values, which may suggest the involvement of distinct interaction mechanisms in the partition process. The correlation with the 137 remaining compounds (i.e., excluding the outliers) is also shown in Table 4. The signs of the coefficients remain unchanged, and their magnitudes are comparable to those in eq 8, with the S term being a little bit less significant. As expected, the statistical parameters have considerably improved.

For all tested correlations where $Y = \log P$, the independent term has no statistical significance. This can be rationalized as follows: for an ideal solute for which B, S, and V approach zero, log P tends to zero and therefore P approaches 1. This means the solute's concentration in both phases becomes very close.

Biological Activity. Various kinds of biological data can be related to lipophilicity parameters.[20,34] Lipophilicity is indeed considered on its own the most informative and successful physicochemical property in medicinal chemistry[20] and has been used in numerous structure–property relationships.[35,36] We have thus searched for a relationship between the biological activity of these compounds, expressed in terms of log(1/MIC) against *M. tuberculosis*, and a set of molecular descriptors X_i, where X_i are the same as those in eqs 5−7:

$$\log(1/\mathrm{MIC}) = a_0 + \sum_{i=1}^{n} a_i X_i \quad (9)$$

The most relevant results are shown in Table 5. The first important conclusion is that in every correlation tested for any set of compounds, we always have $X_i \neq \log P$. We also tested different $\log(^1/_{\mathrm{MIC}}) = f_{\mathrm{nl}}(\mathrm{clogP})$ equations, where f_{nl} represents a nonlinear function and no significant correlation was detected for any set or subset of compounds. This clearly shows that lipophilicity is not an important property to explain the biological response of these compounds. This observation might imply one out of two hypotheses (or both): (i) the penetration process through the cell membrane is not determinant for the antitubercular activity of these com-

Table 1. Abraham's Descriptors for the Tested Compounds

Compd	*A*	*B*	*S*	*E*	*V*	clogP	compd	*A*	*B*	*S*	*E*	*V*	clogP
1	0.543	1.492	2.033	1.155	1.032	−0.67	**98**	0.500	1.040	1.300	1.129	0.099	−0.5
2	0.458	1.570	2.073	1.091	1.595	0.87	**99**	0.451	0.992	1.666	1.018	0.932	−0.28
3	0.458	1.569	2.075	1.092	1.454	0.26	**100**	0.183	1.941	2.388	1.962	1.994	−0.26
4	0.458	1.570	2.073	1.091	1.595	0.78	**101**	0.183	1.949	2.379	1.927	2.135	−0.13
5	0.290	1.310	1.300	1.309	1.768	1.45	**102**	0.183	1.967	2.338	1.912	2.275	0.4
6	0.290	1.350	1.310	1.294	1.909	1.97	**103**	0.864	2.982	3.148	2.394	2.733	−1.24
7	0.290	1.350	1.310	1.294	1.909	1.97	**104**	0.543	1.228	1.827	1.087	1.131	−0.05
8	0.461	1.292	2.300	1.628	1.682	1.31	**106**	0.543	1.243	1.848	1.229	0.997	0.06
9	0.992	2.225	2.337	1.459	1.587	−0.58	**107**	1.084	2.340	3.059	1.765	1.635	−1.4
10	1.054	2.094	3.712	2.283	2.020	−1.16	**108**	0.543	1.191	2.001	1.293	1.336	0.86
11	0.724	1.674	2.775	1.270	1.329	−0.44	**109**	0.290	0.650	0.950	1.145	1.214	0.14
12	0.724	2.025	3.379	1.919	1.755	0.19	**110**	0.290	0.700	1.520	1.279	1.311	0.77
13	0.810	1.800	2.100	2.024	1.920	0.07	**111**	1.084	2.162	2.479	1.130	1.060	−2.53
15	0.290	1.230	1.210	1.019	1.172	−0.17	**112**	1.084	2.209	2.736	0.985	1.103	−2.64
16	0.290	1.240	1.170	1.034	1.313	0.36	**113**	0.600	2.000	1.510	0.975	2.230	0.29
17	0.290	1.240	1.160	1.025	1.454	0.89	**114**	1.084	2.240	2.803	1.172	1.558	−2.54
18	0.290	1.120	1.220	1.062	1.231	0.11	**115**	0.724	1.323	2.171	0.621	0.903	−1.67
19	0.290	1.120	1.220	1.062	1.372	0.64	**116**	0.370	1.000	0.720	0.381	0.606	−1.62
20	0.610	1.280	1.560	1.401	1.131	−0.97	**117**	0.890	1.460	1.830	1.312	1.190	0.08
21	0.770	1.670	2.170	1.342	1.429	−0.8	**118**	0.290	1.140	1.310	1.680	1.401	0.72
22	0.770	1.670	2.170	1.470	1.570	−0.86	**119**	0.701	1.609	2.148	1.898	1.880	1.11
23	0.290	1.890	1.680	1.437	1.695	1.1	**120**	0.195	1.109	2.081	1.766	1.821	3.22
24	0.290	1.010	1.490	1.159	1.154	0.1	**121**	0.661	1.524	1.775	1.287	1.272	−0.23
25	0.290	1.030	1.570	1.631	1.290	0.21	**122**	0.290	1.140	1.300	1.155	1.032	−0.67
26	0.290	1.280	1.890	1.502	1.206	−3.96	**123**	0.543	1.492	2.033	1.155	1.032	−0.32
27	0.290	1.280	1.820	1.813	1.639	1.43	**124**	0.543	1.494	2.032	1.153	1.172	−1.35
28	0.290	1.300	1.820	1.812	1.780	1.4	**125**	0.847	1.622	1.958	0.905	1.161	−2.01
29	0.290	1.210	1.400	1.303	1.270	0.06	**126**	0.543	1.748	1.801	0.794	1.301	−1.55
30	0.790	1.440	1.750	1.644	1.739	1.26	**127**	0.543	1.872	2.460	0.956	1.458	−2.97
31	0.450	1.500	2.100	1.236	1.609	−0.37	**128**	0.543	2.091	2.391	0.941	1.699	−1.7
32	0.400	1.664	1.500	1.252	1.188	−1.73	**129**	0.705	1.278	1.242	0.565	0.979	−1.06
33	0.458	1.566	2.103	1.095	2.722	5.24	**130**	0.543	1.260	2.019	1.479	1.262	–
34	0.458	1.619	2.408	1.556	1.600	−0.11	**131**	0.705	1.346	1.646	1.226	1.305	0.09
35	0.810	1.950	3.798	2.247	2.094	−3.22	**132**	0.925	1.446	2.068	1.141	0.934	−0.53
36	0.543	1.518	2.085	1.030	1.049	−0.47	**133**	0.925	1.498	2.363	1.666	1.444	–
37	0.300	1.010	1.670	1.472	1.207	0.25	**134**	0.951	1.608	2.143	1.149	0.893	−0.99
38	0.458	1.572	2.072	1.090	1.736	1.31	**135**	0.543	1.668	2.219	1.151	1.033	−1.02
39	0.290	1.120	1.500	1.173	1.172	−0.57	**137**	0.951	1.660	2.440	1.675	1.262	0.61
40	0.640	1.190	1.560	1.531	1.131	−0.37	**138**	0.543	1.636	2.131	1.151	0.990	−1.19
41	0.363	1.077	1.535	1.117	1.552	1.27	**139**	1.084	2.633	3.343	1.562	1.347	−3.46
42	1.390	2.667	2.878	1.905	2.127	−2.37	**140**	0.543	1.728	2.144	1.168	0.990	−1.19
43	0.822	1.621	2.872	2.091	2.135	1.04	**141**	0.543	1.415	2.173	1.238	0.956	−0.83
44	0.360	1.060	1.400	1.133	1.270	0.43	**142**	0.543	1.415	2.173	1.238	0.956	−0.48
45	0.360	1.066	1.421	1.127	1.975	3.07	**143**	0.788	1.561	2.638	1.622	1.056	−1.12
46	0.363	1.088	1.673	1.258	2.495	4.71	**144**	0.788	1.561	2.638	1.622	1.056	−0.77
47	0.363	1.071	1.566	1.122	2.538	5.19	**145**	0.543	1.467	2.470	1.764	1.325	1.11
48	0.363	1.069	1.544	1.152	1.411	0.13	**146**	0.691	3.192	1.898	1.601	1.199	−1.09
49	0.363	1.072	1.541	1.149	1.693	1.19	**147**	0.543	1.209	1.722	0.954	0.893	−0.56
50	0.363	1.075	1.539	1.147	1.975	2.25	**148**	0.290	0.800	1.400	1.270	1.068	0.02
51	0.363	1.069	1.916	1.273	1.715	1.33	**149**	0.543	1.339	2.248	1.198	1.067	−3.85
52	0.363	1.086	1.875	1.258	1.866	1.85	**150**	1.084	2.284	2.998	1.454	1.249	−2.1
53	0.363	1.377	2.151	1.789	2.360	3.15	**151**	0.363	0.900	1.200	0.858	1.174	0.09
54	0.363	1.378	2.150	1.788	2.500	3.68	**152**	0.183	1.319	1.579	0.888	1.315	0.97
55	0.363	1.553	2.175	1.952	2.401	3.06	**153**	0.461	1.009	1.989	1.428	1.543	1.98
56	0.363	2.147	2.438	2.037	2.923	3.29	**154**	0.458	1.571	2.572	1.035	1.470	−0.45
57	0.363	1.422	2.034	1.290	1.709	0.1	**155**	0.724	1.391	2.464	1.069	1.190	−0.51
58	1.217	2.370	2.633	1.760	1.928	−2.2	**156**	0.724	1.458	2.757	1.518	1.477	−0.13
59	1.551	2.804	2.918	1.971	2.127	−2.03	**157**	0.363	0.794	1.224	0.916	1.413	1.41
60	2.312	4.116	3.930	2.818	3.158	−3.9	**158**	0.363	0.786	1.233	0.951	1.272	0.06
61	4.103	6.931	3.733	4.091	4.880	−2.69	**159**	0.822	1.337	2.561	1.891	1.996	1.34
83	0.310	1.040	0.950	1.042	1.073	0.26	**160**	1.390	2.383	2.567	1.704	1.988	−2.22
84	0.310	0.900	1.080	1.294	1.195	1.12	**161**	0.543	1.243	1.848	1.229	0.997	0.06
85	0.290	0.740	1.190	1.464	1.248	1.27	**162**	0.458	1.605	2.698	1.310	1.575	0.22
86	0.290	0.720	1.280	1.798	1.331	1.53	**163**	0.461	1.043	2.115	1.703	1.648	2.45
87	0.543	1.332	2.390	1.390	1.247	−3.03	**164**	0.724	1.527	3.010	2.068	1.686	0.53
88	0.543	1.332	2.390	1.390	1.247	−3.03	**165**	0.363	0.828	1.350	1.191	1.518	2.06
89	0.543	1.332	2.390	1.390	1.247	−3.03	**166**	0.363	0.817	1.386	1.201	1.941	3.87
90	0.788	1.432	2.168	1.488	1.172	−0.64	**167**	0.363	0.820	1.359	1.226	1.377	0.73
91	0.641	1.200	2.525	1.522	1.172	−0.04	**168**	0.363	0.826	1.354	1.221	1.941	2.84
92	0.788	1.476	2.304	1.426	1.172	−0.64	**169**	0.363	0.820	1.731	1.348	1.691	1.92
93	0.543	1.589	1.893	1.389	1.454	0.63	**170**	4.103	6.682	3.549	4.165	4.846	−1.9
94	1.193	1.191	2.205	1.336	1.131	−0.06	**171**	1.390	2.418	2.694	1.979	2.093	−1.58
95	0.543	1.184	2.083	1.246	1.272	0.43	**172**	0.874	1.561	2.366	1.518	1.297	−1.1
96	0.984	1.456	2.221	1.348	1.331	−0.27	**173**	0.003	1.839	2.328	1.705	1.494	−3.08
97	1.084	2.277	3.140	1.646	1.429	−1.28	–	–	–	–	–	–	–

Note: There are no calculated descriptors for compounds 14, 62-82, 105 and 136.

pounds; (ii) the measure of lipophilicity by an isotropic lipophilicity parameter such as the *n*-octanol–water partition coefficient[37] is not an adequate model to mimic these specific drug−membrane interactions.

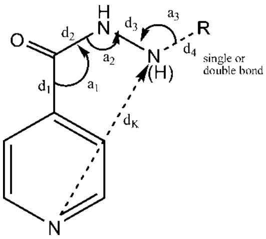

Figure 1. Representation of the geometrical descriptors for isoniazid derivatives.

A close inspection of Table 5 reveals that for only approximately 40% of the analyzed compounds (59 out of 149), the activity against *M. tuberculosis* depends on their basicity and molar volume, the latter being responsible for an increase and the former for a reduction in $\log(^1/_{\mathrm{MIC}})$. When we restrict this set to include only 17 isoniazid derivatives and 13 hydrazides derived from benzoic acid in a total of 30 structurally similar compounds, the following equation is obtained:

$$\log(1/\mathrm{MIC}) = (1.892 \pm 0.142) + (-0.436 \pm 0.091)B + (1.201 \pm 0.126)V \quad (10)$$

$n = 30$; $R^2 = 0.810$; $SD = 0.311$; $F = 58$; $Q^2_{\mathrm{LMO}} = 0.811$

Equation 10 shows that the biological activity of compounds structurally similar to INH depends on their physicochemical characteristics, namely, B and V, independently of the presence or absence of the pyridinic N atom. The same holds true when the analysis is extended to the 59 compounds of Table 5 (eq 12 in the table) and Figure 3 as referred above.

An interesting result was found for the remaining compounds (24 out of the 59 set) without either a pyridinic or a phenylic ring associated with the hydrazide functionality, i.e., for compounds represented by the formula NH_2NHCOR_1, where R_1 can be an aromatic substituent or not but is always distinct from $-C_5NH_4$ and $-C_6H_5$ (5 of the 29 compounds were not included in the regression because they decreased significantly its statistical meaning):

$$\log(1/\mathrm{MIC}) = (2.459 \pm 0.449) + (-0.986 \pm 0.201)B + (-1.703 \pm 0.336)V \quad (11)$$

$n = 24$; $R^2 = 0.773$; $SD = 0.407$; $F = 36$; $Q^2_{\mathrm{LMO}} = 0.785$

A comparison with eq 10 shows that this correlation, although not as statistical meaningful as the previous one, leads to a negative contribution of the molar volume to the biological efficacy. This might indicate that these compounds operate in a deeper zone of the cell membrane than INH related compounds.

The activity of INH derivatives is also fairly well correlated with geometrical and electronic descriptors, particularly those characterizing the hydrazidic moiety of the molecule. From the best correlations presented in eqs 14 and 15 of Table 5, one can see that the distance between the external atom of the hydrazide and the first atom of the R substituent (d_4 in Figure 1) lessens the antitubercular activity of these compounds, whereas both the molecule's dipole moment (μ) and the Mulliken charge (c) on the external hydrazide N atom enhance it (see eq 14). As for the correlations with steric parameters, the results presented in Table 5 (eqs 16 and 17) show that the length (L) of the substituents and the 2D distance between the pyridinic nitrogen and the terminal nitrogen of the hydrazide functionality (d_K) have a positive effect on the activity of INH derivatives while their effective volume (B_5) has a negative effect. Independently of the set of descriptors that best explain the variability in the activity of these compounds, we can say that the model equations shown in Table 5 are capable of predicting values of $\log(^1/_{\mathrm{MIC}})$ to around 0.36 log units.

As stated before, our results give no evidence for a correlation between the biological activity of INH derivatives and their lipophilic properties. This agrees with a study on the activity of isonicotinoylhydrazones for which lipophilicity was also not the critical factor affecting their potency.[24]

Spectroscopic studies on the interaction of tuberculostatics with different liposomes, systems that have been recognized as valuable models of biological membranes,[38] have strongly suggested that INH is located in a very hydrophilic region, operating therefore at the membrane surface. This seems to be in line with the conclusions resulting from the comparison between eqs 10 and 11. On the basis of this evidence, we may infer that in the case of INH derivatives penetration of the compound into the mycobacterial cell wall seems to be less important than binding and/or activation to explain the compounds' biological activity.

Several proposals have been put forward to rationalize the inhibitory action of INH in the synthesis of mycolic acids that form the mycobacterial cell wall. In addition to the mechanisms of action based on the production of INH from the hydrolysis of hydrazones or from the dealkylation of *N*-alkyl substituted INH derivatives, as proposed by Klopman et al.,[11] and in addition to those based on the enzymatic oxidation of INH to INA (isonicotinic acid) inside the cell, followed by its quaternization and incorporation into a NAD analogue which produces a metabolism disorder, thus causing degeneration of bacterial cell wall and ultimately cell death, as suggested by Seydel et al.,[12] other mechanistic paths have been recently proposed.[5–10,39–46] These involve the formation of a isonicotinoyl acyl radical, which results from the activation of INH by the catalase peroxidase of *M. tuberculosis* (CP-KatG), followed by its coupling to NADH (or NAD^+). The exact binding site of INH to the CP-KatG enzyme is still controversial, but recent studies[39–46] strongly suggest that it might be close to the KatG heme pocket, situated in the mtCP N-terminal domain.[43] The INH-NADH (or IN-NAD) adduct, being a powerful inhibitor of InhA, an enoyl−acyl carrier protein reductase involved in mycobacterial cell wall synthesis, also causes a deterioration of the cell wall and in the end its death. The INH-NADH (or IN-NAD) adduct is indeed believed to be the metabolite responsible for the antitubercular activity of INH.[5,40,46]

Our results, based on the application of a QSAR analysis, namely, through eqs 14 and 16, are also consistent with the need of accepting the formation of a radical species in the process of activation of the prodrug, i.e., of the INH derivatives, in addition to recognizing the importance of the hydrazide group in this process, particularly when this group contains a R substituent with relevant electronic and/or steric characteristics. In fact, substituents at the hydrazide moiety may enhance the efficacy of the prodrug by promoting the formation of the isonicotinoyl acyl radical. However, the way in which R operates seems to be distinct in hydrazines and hydrazones INH derivatives (eqs 18–20 in Table 6).

As can been seen from Table 6, the efficacy of the hydrazine prodrugs is favored by the charge over the hydrazinic external N atom (c) but is reduced by the distance between this atom and R (d_4) (eq 18). On the other hand, there is no significant correlation between the activity of these compounds and the steric parameters that characterize their substituents. However, recent reports[40,45,46] show that access to the heme active site of

Table 2. Verloop's Parameters for R and Dipole Moments for All Tested Compounds

	Compd	*L*	*B5*	*B1*	μ (D)
	1	2.185	1.170	1.170	3.44390
	2	5.065	4.621	1.700	5.35094
	3	4.248	3.332	2.062	4.53640
	4	5.058	3.655	2.062	4.98349
	5	4.362	5.098	2.057	6.51530
	6	4.496	5.098	2.057	6.96003
	7	4.362	6.120	2.057	6.99320
	8	5.249	6.667	2.075	2.92880
	9	4.690	4.571	2.384	3.41520
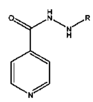	**10**	7.438	6.736	2.265	5.69620
	11	4.330	3.305	1.700	6.33695
	12	6.169	5.558	1.700	2.36269
	13	7.149	5.838	2.275	6.97842
	14	11.614	7.752	1.739	13.79940
	30	5.512	4.448	1.892	2.83932
	31	4.248	4.131	2.902	8.61053
	32	3.461	2.572	1.700	4.33529
	33	14.187	11.093	1.704	11.47650
	34	5.163	5.467	1.702	7.36882
	35	8.180	7.413	2.272	16.06740
	38	5.058	3.655	2.063	6.45792
	15	3.039	2.199	1.700	3.83480
	16	4.278	3.326	1.700	3.45234
	17	5.088	3.648	1.700	3.54603
	18	4.096	3.231	1.520	2.39048
	19	4.906	3.543	1.520	1.97299
	20	3.007	2.043	1.550	3.94309
	21	4.735	4.461	1.550	6.28813
	22	6.452	4.353	1.700	7.85836
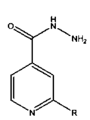	**23**	5.296	3.220	2.061	4.24370
	24	3.470	1.770	1.770	3.48550
	25	4.110	2.060	2.060	3.42076
	26	3.466	2.670	1.550	10.93130
	27	6.284	3.152	1.770	3.48007
	28	5.918	6.085	1.700	3.34405
	29	4.394	3.271	1.700	3.32513
	36	2.791	1.470	1.470	3.75624
	37	3.805	1.920	1.920	3.43203
	39[a]	3.093	2.212	1.700	3.72170
	40[a]	2.915	2.124	1.550	3.37310
	41	4.286	3.332	2.064	6.60530
	42	8.312	5.875	1.895	13.58290
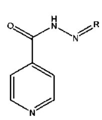	**43**	8.999	4.462	1.876	11.14202
	44	3.044	2.199	1.700	4.16525
	45	8.382	6.112	1.700	11.43620
	46	12.309	10.226	1.700	16.66968
	47	8.382	10.987	1.700	17.61917
	48	4.268	3.250	2.061	5.19137
	49	4.268	4.476	2.655	6.06598
	50	5.995	6.461	2.071	8.11558
	51	5.778	3.668	2.100	7.66146
	52	6.663	4.518	2.094	8.77709
	53	10.421	4.604	1.939	9.86616
	54	11.230	4.683	1.940	10.70450
	55	9.561	3.221	2.062	9.81826
	56	12.305	4.916	2.069	4.15276
	57	6.274	3.475	2.061	7.62397
	58	7.164	5.064	1.891	15.21756
	59	6.508	6.779	2.267	15.66870
	60	10.421	9.892	1.784	20.88980
	61	13.814	8.430	3.402	3.99780
	62	7.951	5.917	2.084	2.84378
	63	7.947	6.270	1.985	2.58587
	64	9.139	5.017	1.887	3.08622
	65	7.950	5.022	1.892	4.55566
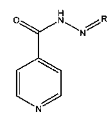	**66**	9.329	5.031	1.894	4.46255
	67	9.581	5.098	1.881	15.09380
	68	6.537	8.834	2.062	4.47664
	69	6.550	10.071	2.036	1.75200
	70	6.546	12.670	2.032	4.75285
	71	6.560	10.154	2.029	1.67207
	72	6.552	9.842	2.042	2.24072
	73	6.548	9.560	2.055	2.24072
	74	6.543	9.221	2.172	19.48466
	75	6.564	9.746	1.981	11.66940
	76	6.567	10.418	1.990	9.60195
	77	6.596	11.638	1.972	5.80908
	78	10.852	17.095	2.065	5.74408
	79	11.586	16.991	2.060	4.61023
	80	6.566	11.523	2.011	1.88280
	81	6.578	14.138	1.999	5.48760
	82	6.571	12.208	1.992	4.05250
	83	2.103	1.000	1.000	4.38695
	84	3.496	1.770	1.770	3.53123
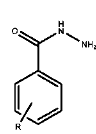	**85**	3.818	1.920	1.920	3.72749
	86	4.145	2.060	2.060	3.75454
	87	3.550	2.611	1.550	11.55613

Table 2. Continued

	Compd	*L*	*B5*	*B1*	μ (D)
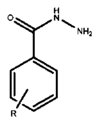	**88**	3.553	2.612	1.550	7.42600
	89	3.466	2.649	1.550	9.13748
	90	2.927	2.116	1.550	2.25404
	91	2.940	2.114	1.550	3.47815
	92	2.927	2.116	1.550	1.83554
	93	4.311	3.277	1.550	4.91088
	94	2.799	2.085	1.520	0.61972
	95	4.297	3.181	1.520	1.84747
	96[b]	---	---	---	2.96321
	97	4.955	3.247	1.709	4.67641
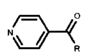	**98**	4.115	2.729	1.550	2.36128
	99	3.070	2.081	1.550	2.48113
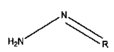	**100**	5.022	7.431	2.194	0.70033
	101	8.444	7.135	2.070	3.94798
	102	8.498	7.297	2.651	2.11259
	103	7.935	10.053	1.797	6.14218
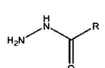	**104**	7.436	4.237	1.700	2.86438
	105	4.748	5.517	1.718	4.78685
	106	5.199	3.164	1.779	4.98986
	107	8.674	4.407	2.024	10.62420
	108	4.679	7.447	1.729	4.89778
	109	4.636	6.089	1.727	5.62630
	110	8.396	4.566	1.700	4.02603
	111	7.035	3.703	1.907	2.00783
	112	4.334	5.884	1.730	5.11445
	113	15.938	9.198	2.105	0.59794
	114	4.759	8.119	2.105	6.71214
	115[b]	---	---	---	3.65731
	116	2.283	1.170	1.170	3.35378
	117	6.027	4.459	1.847	4.03950
	118	6.666	5.560	1.770	2.55064
	119	6.211	6.234	2.610	2.49486
	120[b]	---	---	---	5.41296
	121	4.968	5.999	1.958	2.12363
	122	6.126	3.195	1.779	4.97765
	123	6.147	3.276	1.773	5.24434
	124	4.905	5.655	1.727	3.89023
	125	4.409	4.944	2.096	3.96225
	126	5.627	4.644	2.092	3.77222
	127	5.390	6.754	2.102	5.85143
	128	7.084	7.620	2.101	3.67751
	129	5.139	4.011	1.944	5.53910
	130	7.719	3.560	1.771	6.45510
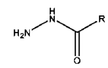	**131**	7.782	5.132	1.700	7.82688
	132	5.294	3.160	1.770	5.54595
	134	5.204	3.142	1.770	4.89734
	135	5.297	4.072	1.876	8.00199
	136	6.598	3.907	1.770	3.16966
	137	7.586	3.543	1.770	8.02139
	138	6.049	3.198	1.770	2.76777
	139	6.045	6.490	1.770	1.59896
	140	5.099	3.205	1.770	1.43985
	141	5.740	3.143	1.771	3.86568
	142	5.007	3.175	1.771	5.49941
	143	6.819	3.142	1.777	3.96327
	144	6.281	3.948	1.771	5.18904
	145	8.029	3.878	1.770	6.63490
	146	6.901	5.505	1.729	4.29650
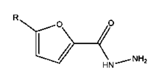	**147**	2.102	1.000	1.000	7.48367
	148	3.783	1.920	1.920	7.54875
	149	3.537	2.618	1.550	17.85851
	150	4.948	3.238	1.712	10.59166
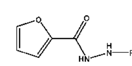	**151**[b]	---	---	---	7.49197
	152[b]	---	---	---	8.56438
	153[b]	---	---	---	5.22405
	154	4.345	4.132	2.925	9.47918
	155	4.344	3.305	1.700	7.74018
	156	5.607	5.272	1.700	9.03736
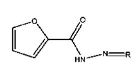	**157**	4.901	3.781	1.853	13.09009
	158	3.953	3.370	2.064	10.92894
	159	6.897	8.851	1.700	11.23660
	160	8.373	6.847	1.776	17.31178
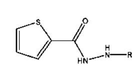	**161**	2.185	1.170	1.170	6.88857
	162	4.283	4.083	2.906	12.19879
	163[b]	---	---	---	8.94785
	164	5.386	5.459	1.700	9.03715
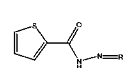	**165**	4.893	3.774	1.854	4.82540
	166	8.672	7.075	1.700	17.69532
	167	3.950	3.370	2.065	5.44076
	168	6.463	7.602	1.885	16.87788
	169	5.074	5.697	1.700	14.64358
	170	8.026	12.879	1.925	22.38454
	171	8.290	6.923	1.761	17.84785
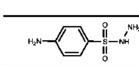	**172**[b]	---	---	---	9.30823
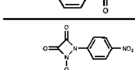	**173**[b]	---	---	---	13.95354

[a] R in position 3 of the pyridinic ring. [b] Compounds **96**, **115**, **120**, **151**−**153**, and **163** have no assigned Verloop's parameters because they have more than one substituent. Compounds **172** and **173** do not have a substituent.

Table 3. Geometrical and Electronic Descriptors for INH Related Compounds

	distance (Å)					angle (deg)			dihedral angle RNN(CO) (deg)	Mulliken charge
Compd	d_k	d_1	d_2	d_3	d_4	a_1	a_2	a_3	a_4	
1	6.35100	1.36100	1.38530	1.37810	0.00000	119.839	119.839	109.916	116.374	−0.66710
2	6.31769	1.36005	1.38660	1.38187	1.45692	119.995	120.152	111.663	223.627	−0.46829
3	6.31195	1.35998	1.38709	1.38090	1.45948	119.991	119.860	113.037	239.422	−0.46624
4	6.31124	1.35989	1.38714	1.38075	1.46110	119.994	119.811	113.363	239.454	−0.46597
5	6.31722	1.36012	1.38621	1.38130	1.45677	119.991	120.311	111.508	119.438	−0.46817
6	6.31760	1.36015	1.38646	1.38152	1.45697	119.986	120.358	111.506	119.832	−0.46817
7	6.31725	1.36017	1.38645	1.38166	1.45687	119.991	120.309	111.544	237.292	−0.46817
8	6.27008	1.36083	1.39145	1.35074	–	119.961	124.637	–	–	−0.36459
9	6.31400	1.36018	1.38614	1.38021	1.45242	119.998	119.625	108.514	232.652	−0.41852
10	6.32043	1.35962	1.38934	1.38013	1.77881	120.004	120.816	113.840	289.529	–
11	6.09528	1.35618	1.37714	1.34646	1.44344	120.019	114.085	73.680	127.219	−0.37345
12	6.09878	1.35943	1.38352	1.34967	1.44869	120.003	115.458	119.680	129.067	−0.37237
13	6.31950	1.35956	1.38929	1.37996	1.77852	119.999	120.833	113.931	289.278	–
14	4.99342	1.36178	1.38823	1.35131	1.44936	120.010	123.297	75.975	257.760	−0.37944
15	4.91679	1.36168	1.38674	1.37817	1.01500	119.972	123.672	108.961	116.397	−0.66708
16	4.92031	1.36177	1.38672	1.37805	1.01490	119.976	123.677	108.964	116.884	−0.66708
17	4.92481	1.36187	1.38670	1.37805	1.01498	119.982	123.723	108.968	116.873	−0.66708
18	4.91927	1.36212	1.38702	1.37805	1.01502	119.979	123.778	108.957	116.378	−0.66708
19	4.91702	1.36211	1.38690	1.37807	1.01492	119.978	123.772	108.964	116.393	−0.66708
20	4.91085	1.36192	1.38687	1.37803	1.01496	119.977	123.730	109.032	116.210	−0.66708
21	4.87703	1.36167	1.38731	1.37869	1.01507	119.961	123.644	108.812	116.519	−0.66708
22	4.91250	1.36162	1.38671	1.37835	1.01537	119.976	123.646	108.775	116.414	−0.66708
23	4.85915	1.36186	1.38668	1.37857	1.01494	119.953	123.368	109.039	117.047	−0.66708
24	4.92180	1.36152	1.38681	1.37820	1.01485	119.973	123.687	108.966	116.468	−0.66708
25	4.92066	1.36171	1.38692	1.37812	1.01493	119.968	123.678	108.983	116.522	−0.66708
26	4.92523	1.36200	1.38677	1.37827	1.01496	119.965	123.666	108.960	116.365	−0.66707
27	4.87205	1.36167	1.38688	1.37842	1.01512	119.960	123.558	108.981	116.716	−0.66708
28	4.92460	1.36194	1.38679	1.37803	1.01490	119.985	123.779	108.947	116.608	−0.66708
29	4.90364	1.36208	1.38679	1.37818	1.01493	119.974	123.651	108.969	116.462	−0.66708
30	4.98419	1.36247	1.38856	1.37654	1.45531	119.996	124.630	114.406	231.999	−0.42710
31	4.99430	1.36330	1.38955	1.37869	1.45865	119.997	124.751	111.801	236.571	−0.42694
32	5.45915	1.35997	1.39000	1.35009	1.37522	119.980	102.291	116.622	184.633	−0.38205
33	4.94580	1.36208	1.38786	1.37934	1.45572	119.974	123.697	111.432	134.419	−0.46852
34	4.96502	1.36211	1.38787	1.37930	1.45356	119.979	124.293	110.817	137.057	−0.43615
35	6.31953	1.35967	1.38926	1.37995	1.77851	120.004	120.831	113.977	289.213	–
36	4.92580	1.36156	1.38692	1.37805	1.01503	119.972	123.723	108.991	116.466	−0.66708
37	4.92440	1.36167	1.38670	1.37811	1.01486	119.975	123.703	109.020	116.458	−0.66708
38	4.96460	1.36203	1.38747	1.37913	1.46228	119.977	124.295	112.070	240.479	−0.46571
39	4.86318	1.35945	1.38472	1.37855	1.01505	119.801	121.868	108.810	116.139	−0.66708
40	4.89430	1.36093	1.38513	1.37721	1.01416	119.891	122.504	110.052	115.668	−0.66709
41	6.13292	1.35948	1.35107	1.23178	1.26300	116.756	125.779	121.220	179.460	−0.35907
42	6.13250	1.35972	1.35110	1.23173	1.26319	116.700	125.988	121.050	178.942	−0.35510
43	6.13840	1.35978	1.35134	1.23243	1.26391	116.958	125.738	121.841	180.000	−0.34409
44	6.13070	1.35955	1.35101	1.23182	1.26314	116.627	125.998	121.075	180.000	−0.35971
45	6.12865	1.35953	1.35075	1.23174	1.26308	116.493	126.241	120.615	180.970	−0.35935
46	6.13044	1.35962	1.35087	1.23183	1.26321	116.583	126.160	120.757	181.646	−0.35935
47	6.13012	1.35948	1.35083	1.23176	1.26319	116.570	126.176	120.709	181.634	−0.35935
48	6.12705	1.35962	1.35115	1.23040	1.26266	116.498	125.780	125.144	180.066	−0.35659
49	6.13251	1.35968	1.35188	1.22880	1.26172	116.945	124.644	130.141	180.077	−0.35596
50	6.13125	1.35917	1.35126	1.22994	1.26164	116.961	124.406	126.554	180.636	−0.35624
51	6.12439	1.35968	1.35092	1.23029	1.26244	116.295	126.246	124.427	179.972	−0.35599
52	6.12621	1.35975	1.35105	1.23033	1.26229	116.395	126.111	124.529	179.956	−0.35599
53	6.13906	1.35973	1.35133	1.23234	1.26356	117.066	125.346	122.251	180.143	−0.34409
54	6.13120	1.35930	1.35115	1.23154	1.26354	116.754	125.493	122.142	180.492	−0.34409
55	6.13325	1.35951	1.35121	1.23196	1.26372	116.766	125.771	121.755	180.590	−0.34409
56	6.13355	1.35942	1.35118	1.23187	1.26354	116.833	125.545	121.966	181.333	−0.34409
57	6.13014	1.35969	1.35115	1.23047	1.26302	116.646	125.727	125.349	179.094	−0.35290
58	6.13279	1.35965	1.35104	1.23188	1.26325	116.714	125.998	121.079	179.191	−0.35510
59	6.12471	1.35994	1.35087	1.23026	1.26366	116.233	126.596	124.503	177.451	−0.34409
60	6.14119	1.35958	1.35310	1.23166	1.26392	117.683	123.583	125.480	181.149	−0.35510
61	6.0487	1.35266	1.34489	1.22150	1.29149	114.296	122.545	123.943	178.678	−0.35401
62	6.12982	1.35990	1.35092	1.23208	1.26358	116.441	126.687	120.242	180.426	−0.35417
63	6.12902	1.35980	1.35082	1.23202	1.26334	116.420	126.633	120.306	180.311	−0.35417
64	6.12926	1.35982	1.35094	1.23204	1.26340	116.424	126.604	120.364	180.219	−0.35417
65	6.13029	1.35991	1.35094	1.23220	1.26343	116.489	126.561	120.434	180.173	−0.35417
66	6.13092	1.35996	1.35110	1.23214	1.26341	116.493	126.583	120.480	180.143	−0.35417
67	6.12932	1.35972	1.35086	1.23186	1.26328	116.464	126.537	120.389	180.097	−0.35417
68	6.12985	1.35967	1.35147	1.23029	1.26599	116.722	125.026	128.940	179.928	−0.34409
69	6.12789	1.35976	1.35134	1.23045	1.26635	116.493	125.683	128.230	179.790	−0.34665
70	6.12736	1.35996	1.35110	1.23059	1.26643	116.397	126.050	127.749	179.666	−0.34665
71	6.12750	1.36014	1.35110	1.23070	1.26674	116.346	126.246	127.784	179.779	−0.34409
72	6.12749	1.36005	1.35126	1.23067	1.26666	116.366	126.122	127.937	179.907	−0.34409
73	6.12749	1.36005	1.35126	1.23067	1.26666	116.366	126.122	127.937	179.799	−0.34409

Table 3. Continued

	distance (Å)					angle (deg)			dihedral angle RNN(CO) (deg)	Mulliken charge
Compd	d_k	d_1	d_2	d_3	d_4	a_1	a_2	a_3	a_4	
74	6.13224	1.36007	1.35152	1.23085	1.26653	116.689	125.434	128.660	179.178	−0.34409
75	6.12737	1.36014	1.35110	1.23075	1.26669	116.327	126.274	127.719	179.918	−0.34409
76	6.12765	1.36019	1.35118	1.23073	1.26682	116.335	126.307	127.749	179.758	−0.34409
77	6.12842	1.36025	1.35114	1.23086	1.26684	116.342	126.413	127.449	179.499	−0.34409
78	6.13064	1.36016	1.35143	1.23084	1.26670	116.537	125.878	128.217	179.761	−0.34409
79	6.12907	1.35986	1.35146	1.23042	1.26629	116.602	125.403	128.688	180.372	−0.34409
80	6.12615	1.35999	1.35109	1.23052	1.26666	116.278	126.314	127.746	179.524	−0.34409
81	6.12837	1.35998	1.35115	1.23059	1.26648	116.440	125.941	128.013	179.568	−0.34409
82	6.12543	1.35991	1.35098	1.23046	1.26645	116.257	126.283	127.682	178.998	−0.34409

Table 4. $\log P = a_1B + a_2S + a_3V$

Compd's family		$a_1 \pm s(a_1)$	$a_2 \pm s(a_2)$	$a_3 \pm s(a_3)$	n	AE^a	AAE^b	SD	R^2	R_0^2	Q^2_{LOO}	Q^2_{LMO}	F
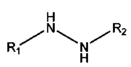	TOTAL SET	-2.218 ± 0.116	-0.258 ± 0.089	2.657 ± 0.116	137	---	---	0.665	0.815	---	0.814	0.814	197
	TRAINING SET	-2.254 ± 0.149	-0.203 ± 0.112	2.651 ± 0.130	98	---	---	0.665	0.830	---	0.825	0.814	154
	TEST SET	---	---	---	39	-0.191	0.547	0.661	0.776	0.756	0.788	---	---
	TRAINING SET	-2.416 ± 0.120	----	2.562 ± 0.121	98	---	---	0.673	0.824	---	0.819	0.818	224
	TEST SET	---	---	---	39	-0.201	0.575	0.693	0.754	0.732	0.763	---	---
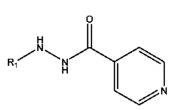	TOTAL SET	-2.327 ± 0.167	-0.509 ± 0.158	3.052 ± 0.187	43	---	---	0.655	0.893	----	0.876	0.882	112
	TRAINING SET	-2.298 ± 0.192	-0.456 ± 0.209	3.020 ± 0.250	24	---	---	0.658	0.910	---	0.888	---	71
	TEST SET	---	---	---	19	-0.253	0.570	0.652	0.871	0.847	0.855	---	---

[a] Average error. [b] Average absolute error.

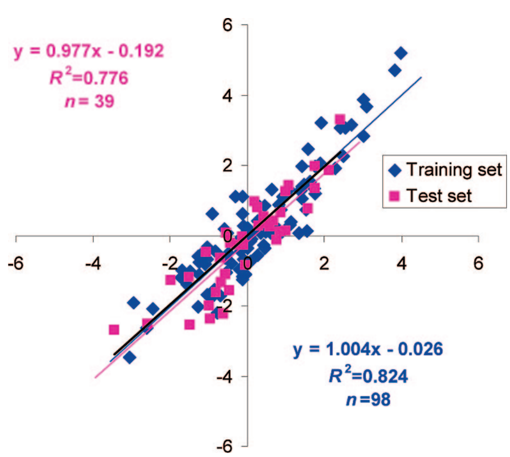

Figure 2. Plot of $\log P_{exp}$ vs $\log P_{calc}$ from eq 8.

KatG presents very strong steric constraints, and therefore, any factor affecting the stereochemistry of these compounds should be very relevant. The observation that even INH derived hydrazines with small volume substituents (e.g., compounds **11**, **15**, **39**, and **40** in Table S1) have very low biological activities by comparison with INH itself confirms this inference.

Table S1 includes 82 INH derivatives, of which 40 are substituted hydrazines, and from these only 8 (compounds **2**−**4**, **9**, **14**, **30**, **31**, and **33**) show MIC values comparable to that of INH. The remaining hydrazines have MIC values 150−160.000 times higher than INH. A close structural inspection of the 8 most active hydrazines, all of them substituted in the hydrazinic moiety, reveals that (i) the 4 most active compounds (compounds **9**, **14**, **30**, and **31**) have a substituent in the hydrazinic moiety with a strong ability to accommodate/delocalize electronic charge and, rather surprisingly, (ii) the remaining 4 hydrazines (compounds **2**−**4** and **33**) possess an aliphatic alkyl substituent, either with a linear or with a branched chain.

On the basis of our QSARs results and on the SARs analysis just described, we can infer that there must be a balance between electronic and steric factors in the activation process of INH derived hydrazines where the specific characteristics of the substituents promote the formation of the acyl radical, provided that the stereochemistry of the prodrug does not obstruct its approximation to the heme site of KatG. This ability to enhance

Table 5. $\log(^1/_{MIC}) = a_0 + a_1X_1 + a_2X_2 + a_3X_3$

Compd's family		a_0 ± $s(a_0)$	a_1 ± $s(a_1)$	a_2 ± $s(a_2)$	a_3 ± $s(a_3)$	n	AE	AAE	SD	R^2	R_0^2	Q^2_{LMO}	F	Eq.
Correlation with Abraham's parameters														
	TOTAL SET	-1.726 ± 0.095	(-0.392 ± 0.064) B	(1.081 ± 0.086) V	----	59	---	---	0.326	0.773	----	0.773	96	[12]
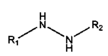	TRAINING SET	-1.770 ± 0.137	(-0.293 ± 0.082) B	(0.984 ± 0.120) V	----	30	---	---	0.320	0.758	----	0.759	42	[13]
	TEST SET	---	---	---	---	29	0.074	0.294	0.350	0.774	0.763	0.764	--	---
Correlation with electronic and geometrical parameters														
	TOTAL SET	4.896 ± 1.032	(0.049 ± 0.013) μ	(5.291 ± 0.685) c	(-2.301 ± 0.638) d_4	33	---	---	0.342	0.812	---	0.813	42	[14]
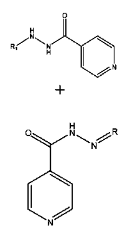	TRAINING SET	4.637 ± 1.286	(0.042 ± 0.016) μ	(5.177 ± 0.892) c	(-2.101 ± 0.778) d_4	22	---	---	0.356	0.805	----	0.805	25	[15]
	TEST SET	---	---	---	---	11	0.053	0.294	0.342	0.835	0.831	0.817	--	---
Correlation with steric parameters														
	TOTAL SET	-6.583 ± 0.646	(0.130 ± 0.031) L	(-0.146 ± 0.018) B_5	(1.206 ± 0.129) d_K	33	---	---	0.306	0.849	---	0.850	54	[16]
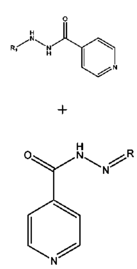	TRAINIG SET	-6.342 ± 0.903	(0.153 ± 0.057) L	(-0.149 ± 0.025) B_5	(1.149 ± 0.190) d_K	22	---	---	0.335	0.830	---	0.900	29	[17]
	TEST SET	---	---	---	---	11	-0.131	0.222	0.263	0.896	0.873	0.942	---	---

the efficacy of these compounds against *M. tuberculosis* might occur, therefore, by a process in which the formation of the precursor (the hydrazyl radical) of the ultimate active agent (the acyl radical) is facilitated by stabilization through resonance, in cases in which it is possible to delocalize electronic charge, or through hyperconjugation, in the presence of linear or branched aliphatic alkyl substituents (Figure 4a).

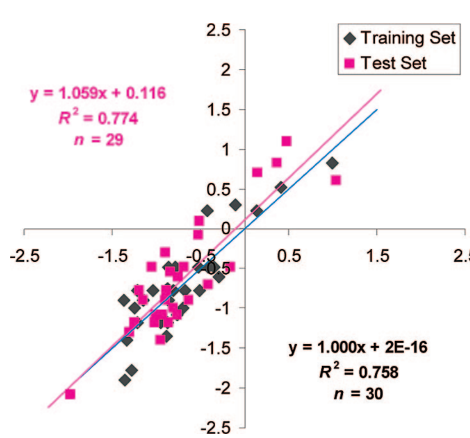

Figure 3. Experimental vs calculated values for $\log(^1/_{MIC}) = f_1(B,V)$, according to eq 13.

For INH derived hydrazones, eq 20 shows that in this case the biological activity does depend on the substituent steric features, showing for the substituent's length (L) a slight positive effect and for its volume (B_5) a negative effect over log(1/*MIC*). Also, in contrast with what was seen for hydrazines, the electronic factors c and μ contribute unfavorably for the activity of these compounds (eq 19). From the 42 INH derived hydrazones included in Table S1, 16 of them (compounds **41**, **43–45**, **48–54**, **56**, **58–61**) show an activity similar to INH and the remaining show MIC values 50−750 higher than INH. An analysis of the structural features of the most active hydrazones discloses a large discrepancy in the characteristics of the hydrazinic substituent. Even compounds with rather big substituents and significant stereochemical constraints (i.e., com-

Table 6. $\log(^{1}/_{\mathrm{MIC}}) = a_0 + a_1X_1 + a_2X_2 + a_3X_3$

Compd's family		$a_0 \pm s(a_0)$	$a_1 \pm s(a_1)$	$a_2 \pm s(a_2)$	$a_3 \pm s(a_3)$	*n*	*SD*	R^2	Q^2_{LMO}	*F*	Eq.
Correlation with electronic and geometrical parameters											
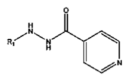	TOTAL SET	10.519 ± 1.716	---	(13.483 ± 1.779) *c*	(-2.721 ± 0.669) d_4	31	0.690	0.705	0.708	33	[18]
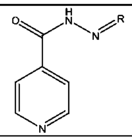	TOTAL SET	-36.878 ± 4.196	(-0.030 ± 0.014) μ	(-107.891 ± 12.051) *c*	---	33	0.408	0.728	0.754	40	[19]
Correlation with steric parameters											
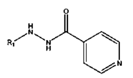	TOTAL SET	---	-----	-----	---	---	---	----	----	-	----
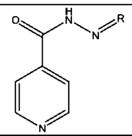	TOTAL SET	1.532 ± 0.321	(0.076 ± 0.040) *L*	(-0.164 ± 0.023) B_5	----	39	0.518	0.590	0.681	26	[20]

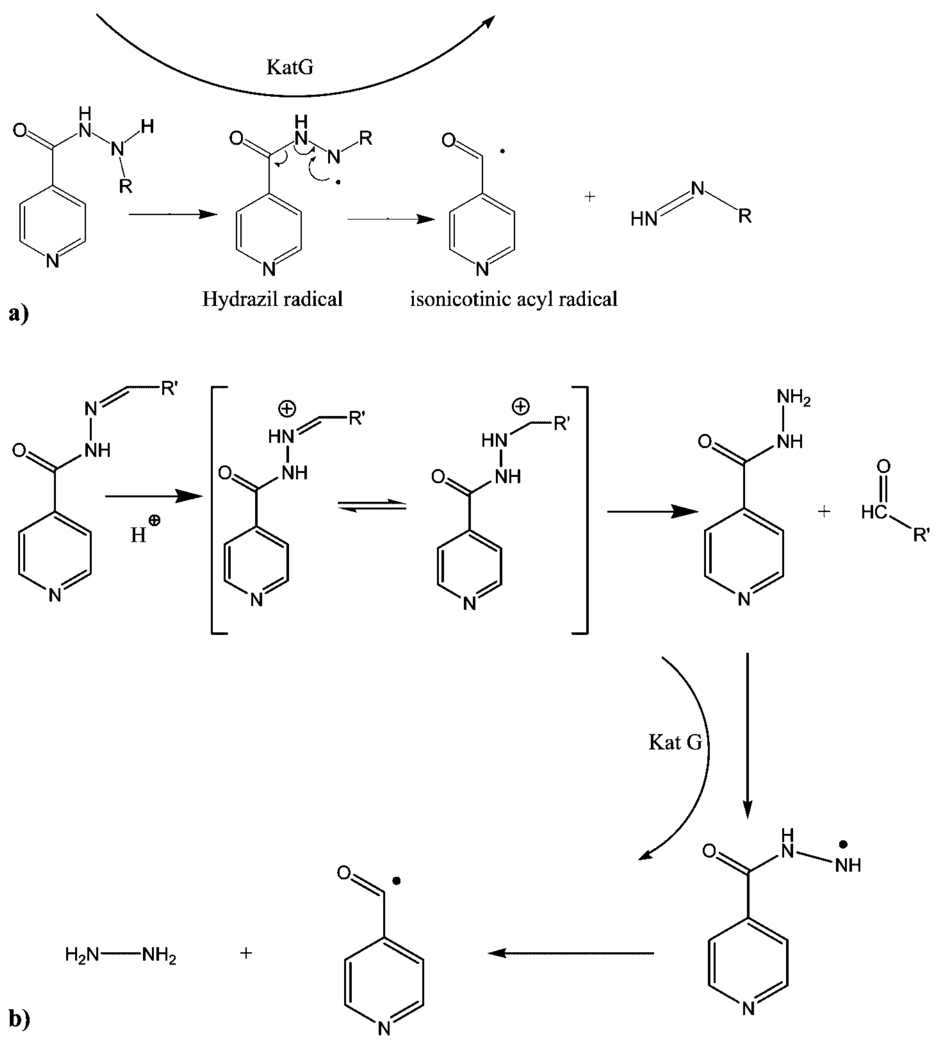

Figure 4. Schematic activation of INH related compounds with the formation of two radical species: (a) subset of INH derived hydrazines; (b) subset of INH derived hydrazones.

pounds **56**, **60**, and **61**) show activities of the same order of magnitude as INH.

The fact that our QSAR analyses show that the activity of these compounds is decreased by electronic factors (c and μ), allied with the information retrieved from SARs and the impossibility of these compounds to form the hydrazyl radical, indicate that the activation of these prodrugs should not be analogous to that of INH derived hydrazines and particularly should not be able to occur near the heme active site of KatG.

These aspects lead us to believe that these compounds go through an initial process of hydrolysis, producing INH and the respective ketone. The produced INH will then follow its activation process catalyzed by KatG, as illustrated in Figure 4b.

The hypothesis of an initial hydrolysis reaction, as already suggested by Klopman et al.,[11] is reinforced by our QSAR results, since the increase in the external N atom charge (c) and the higher dipolarity of the molecule (μ), as well as the higher steric constraint due to the increase of volume of R (B_5), do not favor nucleophilic attack on the protonated hydrazone, therefore reducing the production of INH and, consequently, the biological efficacy of the hydrazone.

Conclusions

The QSAR/QSPR methodology proved to be suitable for predicting the biological activity against *M. tuberculosis* of R_1NHNHR_2 compounds and also for rationalizing the interaction mechanisms involved.

The results clearly show that, in contrast to what was expected, the antitubercular activity of these compounds does not depend on their lipophilic characteristics and that binding and activation seem to be the most relevant steps in the pharmacological processes of these prodrugs.

It is postulated that the activation of INH derivatives' prodrugs (hydrazines and hydrazones) occurs near the surface of the *M. tuberculosis*, although there is some evidence indicating that other hydrazide derivatives (those without a pyridinic or a phenylic ring associated with the hydrazide moiety) may operate in a distinct region, in a deeper zone of the cell membrane.

The correlations found for isoniazid derivatives and related compounds are consistent with a mechanism of action involving an electrophilic intermediate species (hydrazil radical or ion). The ability of the substituents to stabilize this intermediate should influence the rate of formation of the subsequent species, the acyl radical, which coupled to NADH or NAD^+ originates an adduct responsible for the inhibition of InhA, thus restraining mycobacterial cell wall synthesis.

The activation of INH derived hydrazines seems to be favored by hydrazinic substituents with strong characteristics of charge donation and delocalization and/or by hyperconjugation effects. However, since this binding and activation process seems to be initiated near the heme active site of KatG, a substituent's steric constraints should also be taken into account.

The activation of INH derived hydrazones seems to depend on an initial hydrolysis step.

The rational synthesis of new compounds potentially active against *M. tuberculosis* should therefore involve prodrugs with substituent groups with the referenced characteristics, in order to promote the efficacy of the prodrug. The synthesis of these new drugs should contribute to overcoming problematical aspects related to *M. tuberculosis* KatG mutations, which are considered responsible for INH resistance.

Acknowledgment. We are indebted to Prof. Michael Abraham and Dr. Andreas Zissimos for facilitating access to the Absolv program and for the calculation of Abraham's descriptors. We are also thankful to Profs. Ruben Leitão and Susana Santos, and to Dr. Filipe Agapito for fruitful discussions, and to Prof. Lídia Pinheiro for helping us with the setting-up of the database. C. Ventura gratefully acknowledges financial support from Fundação para a Ciência e Tecnologia, Portugal, through Grant BPD/20743/2004. We are also grateful to the reviewers for their helpful comments and suggestions.

Supporting Information Available: Structures of the 173 compounds analyzed in this work (Table S1). This material is available free of charge via the Internet at http://pubs.acs.org.

References

(1) http://www.who.int/tb/en/ (accessed July 2007).
(2) Zhang, Y. The Magic Bullets and Tuberculosis Drug Targets. *Annu. Rev. Pharmacol. Toxicol.* **2005**, *45*, 529–564.
(3) *Global Tuberculosis Control: Surveillance, Planning, Financing*; WHO Report 2006; World Health Organization: Geneva, 2006.
(4) http://www.stoptb.org/ (accessed July 2007).
(5) Ghiladi, R. A.; Medzihradszky, K. F.; Rusnak, F. M.; Montellano, P. R. O. Correlation between Isoniazid Resistance and Superoxide Reactivity in *Mycobacterium tuberculosis*. *J. Am. Chem. Soc.* **2005**, *127*, 13428–13442.
(6) Scior, T.; Morales, I. M.; Eisele, S. J. G.; Domeyer, D.; Laufer, S. Antitubercular Isoniazid and Drug Resistance of *Mycobacterium tuberculosis*. A Review. *Arch. Pharm. (Weinheim, Ger.)* **2002**, *11*, 511–525.
(7) Wengenack, N. L.; Rusnak, F. Evidence for Isoniazid-Dependent Free Radical Generation Catalyzed by *Mycobacterium tuberculosis* KatG and the Isoniazid-Resistant Mutant KatG(S315T). *Biochemistry* **2001**, *40*, 8990–8996.
(8) Rozwarski, D. A.; Grant, G. A.; Barton, D. H. R.; Jacobs, W. R.; Sacchettini, J. C. Modification of the NADH of the Isoniazid Target (InhA) from *Mycobacterium tuberculosis*. *Science* **1998**, *279*, 98–102.
(9) Ducasse-Cabanot, S.; Cohen-Gonsaud, M.; Marrakchi, H.; Nguyen, M.; Zerbib, D.; Bernadou, J.; Daffé, M.; Labesse, G.; Quémard, A. In Vitro Inhibition of the *Mycobacterium tuberculosis* β-Ketoacyl-Acyl Carrier Protein Reductase MabA by Isoniazid. *Antimicrob. Agents Chemother.* **2004**, *48*, 242–249.
(10) Johnsson, K.; Schultz, P. G. Mechanistic Studies of the Oxidation of Isoniazid by the Catalase Peroxidase from *Mycobacterium tuberculosis*. *J. Am. Chem. Soc.* **1994**, *116*, 7425–7426.
(11) Klopman, G.; Fercu, D.; Jacob, J. Computer-Aided Study of the Relationship between Structure and Antituberculosis Activity of a Series of Isoniazid Derivatives. *Chem. Phys.* **1996**, *204*, 181–193.
(12) Seydel, J. K.; Schaper, K.-J.; Wempe, E.; Cordes, H. P. Mode of Action and Quantitative Structure−Activity Correlations of Tuberculostatic Drugs of the Isonicotinic Acid Hydrazide Type. *J. Med. Chem.* **1976**, *19*, 483–492.
(13) Bagchi, M. C.; Maiti, B. C.; Mills, D.; Basak, S. C. Usefulness of Graphical Invariants in Quantitative Structure−Activity Correlations of Tuberculostatic Drugs of the Isonicotinic Acid Hydrazide Type. *J. Mol. Model.* **2004**, *10*, 102–111.
(14) Saint-Joanis, B.; Souchon, H.; Wilming, M.; Johnsson, K.; Alzari, P. M.; Cole, S. T. Use of Site-Directed Mutagenesis To Probe the Structure, Function and Isoniazid Activation of the Catalase/Peroxidase, KatG, from *Mycobacterium tuberculosis*. *Biochemistry* **1999**, *338*, 753–760.
(15) Wilming, M.; Johnsson, K. Spontaneous Formation of the Bioactive Form of the Tuberculosis Drug Isoniazid. *Angew. Chem., Int. Ed.* **1999**, *38*, 2588–2590.
(16) Nguyen, M.; Quémard, A.; Broussy, S.; Benadou, J.; Meunier, B. Mn(III) Pyrophosphate as an Efficient Tool for Studying the Mode of Action of Isoniazid on the InhA Protein of *Mycobacterium tuberculosis*. *Antimicrob. Agents Chemother.* **2002**, *46*, 2137–2144.
(17) Timmins, G.; Master, S.; Rusnak, F.; Dereic, V. Requirements for Nitric Oxide Generation from Isoniazid Activation in Vitro and Inhibition of Mycobacterial Respiration in Vivo. *J. Bacteriol.* **2004**, *186*, 5427–5431.
(18) Timmins, G.; Master, S.; Rusnak, F.; Dereic, V. Nitric Oxide Generated from Isoniazid Activation by KatG: Source of Nitric Oxide and Activity against *Mycobacterium tuberculosis*. *Antimicrob. Agents Chemother.* **2004**, *48*, 3006–3009.
(19) Shindikar, A. V.; Viswanathan, C. L. Novel Fluoroquinolones: Design, Synthesis, and in Vivo Activity in Mice against *Mycobacterium tuberculosis* $H_{37}R_v$. *Bioorg. Med. Chem. Lett.* **2005**, *15*, 1803–1806.
(20) Testa, B.; Crivori, P.; Reist, M.; Carrupt, P. A. The Influence of Lipophilicity on the Pharmacokinetic Behavior of Drugs: Concepts and Examples. *Perspect. Drug Discovery Des.* **2000**, *19*, 179–211.

(21) (a) Platts, J. A.; Butina, D.; Abraham, M. H.; Hersey, A. Estimation of Molecular Linear Free Energy Relation Descriptors by a Group Contribution Approach. *J. Chem. Inf. Comput. Sci.* **1999**, *39*, 835–845. (b) Abraham, M. H.; Ibrahim, A.; Zissimos, A. M.; Zhao, Y. H.; Comer, J.; Reynolds, D. P. Application of Hydrogen Bonding Calculations in Property Based Drug Design. *Drug Discovery Today* **2002**, *7*, 1056–1063.

(22) Leo, A.; Hansch, C.; Elkins, D. Partition Coefficients and Their Uses. *Chem. Rev.* **1971**, *71*, 525–616.

(23) Mohamad, S.; Ibrahim, P.; Sadikun, A. Susceptibility of *Mycobacterium tuberculosis* to Isoniazid and Its Derivative, 1-Isonicotinyl-2-nonanoyl hydrazine: Investigation at Cellular Level. *Tuberculosis* **2004**, *84*, 56–62.

(24) De Logu, A.; Onnis, V.; Saddi, B.; Congiu, C.; Schivo, M. L.; Cocco, M. T. Activity of a New Class of Isonicotinoylhydrazones Used Alone and in Combination with Isoniazid, Rifampicin, Ethambutol, Para-aminosalicylic Acid and Clofazimine against *Mycobacterium tuberculosis*. *J. Antimicrob. Chemother.* **2002**, *49*, 275–282.

(25) Sriram, D.; Yogeeswari, P.; Madhu, K. Synthesis and in Vivo Antimycobacterial Activity of Isonicotinoyl Hydrazones. *Bioorg. Med. Chem. Lett.* **2005**, *15*, 4502–4505.

(26) Molecular Modeling Pro Plus, version 6.2.5; www.chemistry-software.com.

(27) (a) Chatterjee, S.; Hadi, A. S. Influential Observations, High Leverage Points, and Outliers in Linear Regression. *Stat. Sci.* **1986**, *1*, 379–416. (b) Kim, C.; Storer, B. E. Reference Values for Cook's Distance. *Commun. Stat.—Theory and Methods* **1996**, *25*, 691–708. (c) Kim, C.; Lee, Y.; Park, B. U. Cook's Distance in Local Polynomial Regression. *Stat. Probability Lett.* **2001**, *54*, 33–40. (d) Díaz-García, J. A.; González-Farías, G. A Note on the Cook's Distance. *J. Stat. Planning Inference* **2004**, *120*, 119–136.

(28) (a) Serneels, S.; Croux, C.; Van Espen, P. J. Influence Properties of Partial Least Squares Regression. *Chemom. Intell. Lab. Syst.* **2004**, *71*, 13–20. (b) Militino, A. F.; Palácios, M. B.; Ugarte, M. D. Outliers Detection in Multivariate Spatial Linear Models. *J. Stat. Planning Inference* **2006**, *136*, 125–146.

(29) Eriksson, L.; Jaworska, J.; Worth, A. P.; Cronin, M. T. D.; McDowell, R. W. Methods for Reliability and Uncertainty Assessment and for Applicability Evaluations of Classification- and Regression- Based QSARs. *Environ. Health Perspect.* **2003**, *111*, 1361–1375.

(30) Tropsha, A.; Gramatica, P.; Gombar, V. K. The Importance of Being Earnest: Validation Is the Absolute Essential for Successful Application and Interpretation of QSPR Models. *QSAR Comb. Sci.* **2003**, *22*, 69–77.

(31) Golbraik, A.; Tropsha, A. Beware of q^2! *J. Mol. Graphics. Modell.* **2002**, *20*, 269–276.

(32) (a) Abraham, M. H.; Martins, F.; Mitchell, R. C. Algorithms for Skin Permeability Using Hydrogen Bond Descriptors. *J. Pharm. Pharmacol.* **1997**, *49*, 858–865. (b) Platts, J. A.; Abraham, M. H.; Butina, D.; Hersey, A. Estimation of Molecular Linear Free Energy Relationship Descriptors by a Group Contribution Approach. 2. Prediction of Partition Coefficients. *J. Chem. Inf. Comput. Sci.* **2000**, *40*, 71–80. (c) Zissimos, A. M.; Abraham, M. H.; Barker, M. C.; Box, K. J.; Tam, K. Y. Calculation of Abraham Descriptors from Solvent−Water Partition Coefficients in Four Different Systems; Evaluation of Different Methods of Calculation. *J. Chem. Soc., Perkin Trans. 2* **2002**, 470–477. (d) Abraham, M. H.; Chada, H. S.; Martins, F.; Mitchell, R. C.; Bradbury, M. W.; Gratton, J. A. Hydrogen Bonding Part 46: A Review of the Correlation and Prediction of Transport Properties by an LFER Method: Physicochemical Properties, Brain Penetration and Skin Permeability *Pestic. Sci.* **1999**, *55*, 78–88.

(33) Verloop, A.; Tipker, J. Pharmaco Chemistry Library. In *QSAR in Drug Design and Toxicology*; Hadzi, D., Jorman-Blazic, B., Eds.; Elsevier Science Publishers B.V.: Amsterdam, 1987; Vol. 10; pp 97–125.

(34) Verma, R. P.; Kurup, A.; Mekapati, S. B.; Hansch, C. Bioorg. Chemical−Biological Interactions in Human. *Med. Chem.* **2003**, *13*, 933–948.

(35) (a) Selassie, C. D. History of Quantitative Structure−Activity Relationships, 1. In *Burger's Medicinal Chemistry and Drug Discovery*, 6th ed.; Abraham, D. J., Ed.; John Wiley and Sons: New York, 2003; Vol. 1, pp 1–48. (b) Tropsha, A. Recent Trends in Quantitative Structure−Activity Relationships. In *Burger's Medicinal Chemistry and Drug Discovery*, 6th ed.; Abraham, D. J., Ed.; John Wiley and Sons: New York, 2003; pp 49–76.

(36) Abraham, M. H.; Martins, F. Human Skin Permeation and Partition: General Linear Free-Energy Relationship Analyses. *J. Pharm. Sci.* **2004**, *93*, 1508–1523.

(37) Van Balen, G. P.; Martinet, C. M.; Caron, G.; Bouchard, G.; Reist, M.; Carrupt, P.-A; Fruttero, R.; Gasco, A.; Testa, B. Liposome/Water Lipophilicity: Methods, Information Content, and Pharmaceutical Applications. *Med. Res. Rev.* **2004**, *24*, 299–324.

(38) Rodrigues, C.; Gameiro, P.; Prieto, M.; de Castro, B. Interaction of Rifampicin and Isoniazid with Large Unilamellar Liposomes: Spectroscopic Location Studies. *Biochem. Biophys. Acta* **2003**, *1620*, 151–159.

(39) Wengenack, N. L.; Todorovic, S.; Yu, L.; Rusnak, F. Evidence for Differential Binding of Isoniazid by *Mycobacterium tuberculosis* KatG and the Isoniazid-Resistant Mutant KatG (S315T). *Biochemistry* **1998**, *37*, 15825–15834.

(40) Powers, L.; Hillar, A.; Loewen, P. C. Active Site Structure of the Catalase-Peroxidases from *Mycobacterium tuberculosis* and *Escherichia coli* by Extended X-ray Absorption Fine Structure Analysis. *Biochim. Biophys. Acta* **2001**, *1546*, 44–54.

(41) Wei, C.-J.; Lei, B.; Musser, J. M.; Tu, S.-C. Isoniazid Activation Defects in Recombinant *Mycobacterium tuberculosis* Catalase-Peroxidase (KatG) Mutants Evident in InhA Inhibitor Production. *Antimicrob. Agents Chemother.* **2003**, *47*, 670–675.

(42) Pierattelli, R.; Banci, L.; Eady, N. A. J.; Bodiguel, J.; Jones, J. N.; Moody, P. C. E.; Raven, E. L.; Jamart-Grégoire, B.; Brown, A. Enzyme-Catalyzed Mechanism of Isoniazid Activation in Class I and Class III Peroxidases. *J. Biol. Chem.* **2004**, *279*, 39000–39009.

(43) Bertrand, T.; Eady, N. A. J.; Jones, J. N.; Jesmin; Nagy, J. M.; Jamart-Grégoire, B.; Raven, E. L.; Brown, K. A. Crystal Structure of *Mycobacterium tuberculosis* Catalase-Peroxidase. *J. Biol. Chem.* **2004**, *279*, 38991–38999.

(44) Singh, R.; Wiseman, B.; Deemagarn, T.; Donald, L. J.; Duckworth, H. W.; Carpena, X.; Fita, I.; Loewen, P. C. Catalase-Peroxidases (KatG) Exhibit NADH Oxidase Activity. *J. Biol. Chem.* **2004**, *279*, 43098–43106.

(45) Deemagarn, T.; Carpena, X.; Singh, R.; Wiseman, B.; Fita, I.; Loewen, C. Structural Characterization of the Ser324Thr Variant of the Catalase-Peroxidase (KatG) from *Burkholderia pseudomallei*. *J. Mol. Biol.* **2005**, *345*, 21–28.

(46) Zhao, X.; Yu, H.; Yu, S.; Wang, F.; Sacchettini, J. C.; Magliozzo, R. S. Hydrogen Peroxide-Mediated Isoniazid Activation Catalyzed by *Mycobacterium tuberculosis* Catalase-Peroxidase (KatG) and Its S315T Mutant. *Biochemistry* **2006**, *45*, 4131–4140.

JM701048S